Lightning-Inverse Reconstruction by Remote Sensing and Numerical-Field Synthesis

Andrei Ceclan[1], Vasile Ţopa[1], Dan D. Micu[1], and Amedeo Andreotti[2]

[1]Department of Electrical Engineering, Technical University of Cluj Napoca, Cluj-Napoca 400027, Romania
[2]Department of Electrical Engineering, University of Naples "Federico II", Naples 80123, Italy

An inverse remote-sensing procedure is presented for reconstructing the spatial waveform of the lightning return stroke current throughout a numerical-field synthesis procedure, based on working regularization methods. The approach uses as input data the acquisition of time-domain recordings of the electric and/or magnetic field generated by the lightning current, at various locations on the ground and converts these signals into harmonics by Fourier decomposition. This combination between the proposed solving procedures and harmonic filtering yields numerical results that are in good agreement with the testing functions.

***Index Terms*—Field synthesis, harmonic reconstruction, ill posed, inverse problem, lightning, return stroke current.**

I. Lightning Current Insights

THE evaluation and accurate interpretation of the negative effects that lightning phenomenon has on the environment, power, or communication equipment may be accomplished more easily if the spatial and temporal variation of the return stroke current are known. Lightning effects represent a major problem in electromagnetic compatibility (EMC) [1]–[6].

Thus, there is the opportunity to reconstruct the return stroke current from remotely measured electric and/or magnetic fields which are available because of the widespread use of lightning location systems (LLS) [4], [6].

For this lightning-inverse reconstruction, we adopted the engineering models in which a spatial and temporal distribution of the channel current (or the channel line charge density) is specified based on achieving agreement between the model predicted electromagnetic fields and those observed experimentally at distances from tens of meters to hundreds of kilometers. Engineering return-stroke models have been reviewed by [1], [2], [5], [7], and [8].

Current identified approaches to determine the spatial and temporal waveform of the return stroke current consist in an attempt to match by *trial-and-error* methods the measured field values with the calculated field values, by imposing exponential models (MTLE), square root ones, or linear ones (MTLL) [9], [10]. All of these approaches consist in directly solving the integral equations with the help of the collocation method, using Cebâşev or Geigenbauer base functions, or by artificial-intelligence curve-fitting procedures [11], [12].

II. Technical and Numerical Procedure

A new improved inverse remote-sensing procedure is thus proposed for identifying and reconstructing the spatial and temporal waveform of the lightning return stroke current. It starts with the acquisition of the electric and/or magnetic field generated by the discharge channel, along with its location.

Our identification is performed by using time-domain recording measurements of the electric or magnetic field at various distances from the lightning channel, according to the physical location of the existing LLS. In both cases, we originally propose that the field time-recorded components, to be decomposed by Fourier series and extract some N_ω components from it—amplitudes and phases, if available, apply Fourier series to the time-domain signal of the channel base current too, and extract the same N_ω components from it—amplitudes and phases. By superposing the effect of each frequency signal, an inverse correlation can be stated between the field and lightning current.

Next, for these presented scenarios, we apply the following numerical approach: pass from the analytical integral equation lightning model to a linear system of equations $A \cdot X = u$, through numerical meshing of the spatial variable—channel height on one side, and range of horizontal sensors on the other side. The resulting numerical system of equations has a severely ill-posed solution, a fact expressed by its condition number [13].

III. Engineering Mathematical Approach

There is a wide range of electric or magnetic field synthesis applications that have to be modeled with Fredholm integral equations, as ill-posed inverse problems [13], [14].

Here are the hypothesis that are used in our modelization: the lightning channel is represented as a vertical antenna, along which current propagates as a moving front; the soil is homogeneous, has a flat shape, and perfect conductivity. This way, the kernels of the Fredholm integral equations of the first kind are expressed by rational functions. The geometry model of the lightning reconstruction can be seen above it, where H is the channel height, $i(z',t)$ is the return stroke current spatial and time dependence, and $P(r,\Phi,z)$ is the evaluation location of sensors.

Next, the mathematical expressions of the field components in cylindrical coordinates, both for electric and magnetic fields, as Fredholm integral equations of the first kind are used as the engineering models. The kernels and proofs of these relations are based on Fig. 1, and can be found in [5], [7], [8], and [15]–[17].

Let us introduce the time-dependent vertical component of the electric-field strength, evaluated through dipole theory

$$E_z(r,z,t) = \frac{1}{2\cdot\pi\cdot\varepsilon_0} \cdot \int_0^H \left[\frac{2\cdot(z'-z)^2 - r^2}{R^5} \cdot \int_0^t i(z', \tau - R/c) d\tau \right.$$

Manuscript received November 10, 2012; revised January 01, 2013; accepted January 18, 2013. Date of current version May 07, 2013. Corresponding author: A. Ceclan (e-mail: Andrei.Ceclan@ethm.utcluj.ro).

Color versions of one or more of the figures in this paper are available online at http://ieeexplore.ieee.org.

Digital Object Identifier 10.1109/TMAG.2013.2243425

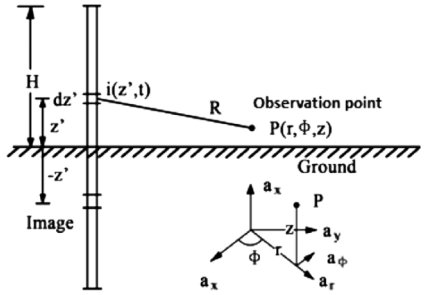

Fig. 1. Geometrical parameters used in calculating return stroke fields.

$$+\frac{2\cdot(z'-z)^2-r^2}{c\cdot R^4}\cdot i(z',t-R/c) -\frac{r^2}{c^2\cdot R^3}\cdot\frac{\partial i}{\partial t}(z',t-R/c)\Bigg]dz'. \quad (1)$$

We found that a misinterpretation persists regarding the frequency domain of these radial, axial, and polar field equations. These do not represent the Fourier transform of the time-domain field expressions, but formally written with complex numbers relations. Thus, (1) converts in (2), and the same applies to the other components

$$E_z(r,z,\omega)=\frac{1}{4\cdot\pi\cdot\varepsilon_0}\cdot\int_{-H}^{H}\Bigg[G_z(r,z,z',\omega) \cdot\exp\left(-j\cdot\omega\cdot\frac{\sqrt{r^2+(z'-z)^2}}{c}\right)\cdot I(z',\omega)\Bigg]dz'. \quad (2)$$

In this case, the kernel function G_z incorporates the static, induction, and radiation contributions, as in correspondence with the relations from (1). The return stroke current (RSC) as a function of (3) and (4) shows dependence to an initial peak value at the channel base, a spatial attenuation along the channel, and to the propagation speed of the current, both for time and frequency dependence

$$i(z',t)=u\left(\frac{t-|z'|}{v}\right)\cdot P(z')\cdot i_0\left(\frac{t-|z'|}{v}\right) \quad (3)$$

$$I(z',\omega)=I(0,\omega)\cdot P(z')\cdot\exp\left(-\frac{j\cdot\omega\cdot|z'|}{v}\right) \quad (4)$$

where ε_0 is the permittivity, j is the imaginary unit, z is the height of the sensor, z' is the spatial variable of the channel height, t is the time variable, ω is the frequency dependence, c is the speed of light, v is the current propagation speed, $R=\sqrt{r^2+(z-z')^2}$, $i_0(t-z'/v)$ is the time domain, and $I(0,\omega)$ is the frequency-converted channel base current (CBC), and $P(z')$ is the spatial attenuation of the return stroke current.

IV. Working Numerical-Field Synthesis Algorithm

Taking into account that this described inverse Fredholm *ill-posed* integral equation consists in computing the cause from the effect, it is expected that small noise in the right-hand-side measured field components, is likely to generate numerical RSCs highly contaminated by undesired high-frequency oscillations [13], [18].

Thus, if one by standard numerical procedures evaluates the solution, this has three major inconvenient characteristics: imprecision, instability to small input field modifications, and physical inconsistence. The ill-posed electromagnetic inverse problems and ill-posed EIP are very well detailed in the literature, especially for Fredholm integral equations [13], [19].

For this reason in our study, the concept of *Working Regularization Algorithm* (WRA) [13] has been adopted as a functional mixture of three factors: 1) a regularization algorithm, 2) a parameter choice method, and 3) the implementation of these methods. For efficiency, we take any available mathematical structure in the problem (singularity, symmetry, sparse) into account.

By using the condition number in the initial evaluation, we can show a clear connection between the solution instability and the condition number, as related to any perturbation that may occur in the measured field, or in the problem structure—the kernel matrix. Thus, the noise acts on the effect–vector as

$$\varepsilon_X[\%]=\frac{\|X'-X\|_2}{\|X\|_2}\le K_A\cdot\frac{\|u'-u\|_2}{\|u\|_2}=K_A\cdot\varepsilon_u[\%] \quad (5)$$

where u' is the perturbed effect vector, $X'$is the resulting solution (attenuation function) as related to the perturbed effect, and K_A is the condition number.

Minimizing a Tikhonov functional [13], [18], expressed with the help of vector norms (6), it is nothing but a constrain method, which limits the uncontrolled growth of the solution

$$f_{\text{Tikhonov}}=\arg\min\{\|A\cdot X-u\|_2+\alpha\cdot\|C\cdot X\|_2\} \quad (6)$$

where A is the matrix system, u is the field vector, $\alpha$is the regularization parameter, and $A\cdot X=u$ is the system of equations originating from the integral (2). The term $\alpha\cdot\|C\cdot X\|$ consists in a penalty applied to the solution, in order to not allow its instability. Also, the operator C may embed geometrical and physical constrains for the solution. This regularization procedure and its derivations may be regarded as a penalty method [13].

The truncated singular value σ_i decomposition (TSVD), applied as a regularization method, with the limitation of certain terms that enter in the sum, as related to a singular value stated as the threshold, is interpreted as being a projection method; an evaluation of a vector by summing up of other vectors, without undesired components

$$X^{(k)}=\sum_{i=1}^{k}f_i\cdot U^{\langle i\rangle^T}\cdot u\cdot V^{\langle i\rangle} \quad (7)$$

where f_i are the filter factors, U,V are the singular matrices, and k is the truncation coefficient which acts as regularization parameter.

Thus, the regularization works either as a penalty method or as a projection one. We classified these regularization procedures as follows: the Tikh is the penalty method, based on Tikhnov theory reflected by relation (6); DVST ON/OFF is the projection method, truncated singular value decomposition with ON/OFF filter factors $f_i=1/\sigma_i\ if\ i\le k\ or\ 0\ if\ i>k$; DVSTA is the projection method, damped truncated decomposition of the singular values, based on relation (7) with $f_i=\sigma_i/(\sigma_i^2+\sigma)\ if\ i\le k\ or\ i>k$; other standard methods are GCS, which is the conjugate gradient method; TRA is the algebraic reconstruction technique [20]; GCV is the generalized cross-validation method expressed as the minimum of $\text{GCV}(\alpha)=\alpha\cdot$

$\partial\|C \cdot X\|^2/\partial\alpha^2$ for the choice of the regularization parameter; and LC is the L-shape curve function with a dependent variation between the error and solution norms as introduced in (6) to which the corner represents the optimum regularization parameter [21].

For each of the aforementioned regularization methods, the original contribution of the authors is related to the definition and evaluation of the filtering factors. The threshold from which the filtering starts is, by itself, a regularization parameter, in relation with the decomposition of the time domain signal.

Both WRA penalty and projection methods consist initially in a harmonic analysis for the norms of the singular vectors V, from the decomposition, and afterwards in a filtering of those singular vectors that have a lower norm, than an imposed limit, if they may be affected by the amplification due to the singular values σ_i, in the solution reconstruction.

After computing the solution, by any of these methods, an error evaluation is performed using the relations

$$E_{\text{solution}}(z') = \frac{|P_{\text{test}}(z') - P(z')|}{|P(z')|} \cdot 100[\%] \tag{8}$$

$$E_{\text{effect}}(r) = \frac{|E_{\text{mas}}(r,z,\omega) - E_{\text{calc}}(r,z,\omega)|}{|E_{\text{mas}}(r,z,\omega)|} \cdot 100[\%]. \tag{9}$$

Some error causes that appear for electric- or magnetic-field measurement: LLS devices and current reflections in instrumented towers [15]. In the evaluations, the sensitivity of the solution is also tested, when noise occurs in the field vector.

V. Numerical Results and Discussions

Not having any available data about the height-dependent attenuation function $P(z')$, the vector X can be numerically evaluated for each frequency from the Fourier spectrum by solving the integral (2) and the other related field integrals. Then, the numerical solutions can be compared with the proposed test functions MTLE and MTLL, since these only have nonunitary spatial attenuation dependence.

Several input data were used regarding the location of the field sensors (range of 50 to 5000 m), the height of the measurement sensors (0 to 15 m), height of the current channel (1 to 7.5 km), and the sampling frequencies of the measured fields (20 to 500 harmonics, related to a maximum duration of 10^{-3} s). All of these numerical cases, applied to the Fredholm integral equation models, vertical electrical field (2), and related horizontal electric- and azimuth magnetic-field strengths, lead to ill-posed and very severely ill-conditioned initial systems of equations and required regularization.

Let us consider the results for a 7.5-km channel height and an initially imposed CBC, as with indicated expressions and parameters given in [4].

In Fig. 2, the result of directly evaluating the electric-field strength for the TL, MTLL, and MTLE models [4], [5], [11] can be seen, both in time domain and the frequency spectrum for the MTLE model, at a distance of 50 m from the strike location, for a duration of 50 μs. This is accounted for in the scenario with only one electric-field sensor for the remote-sensing procedure to identify the spatial distribution of the current along the channel height.

Using these electrical-field values, with 5% additional noise as Fig. 2 shows, we determined the attenuation function by the WRA. In Fig. 3, a sample result is represented for the identification of the MTLE (Test 1) model.

Having the reconstructed MTLE model spatial attenuation function with the Tikhonov using the L curve criterion and 75

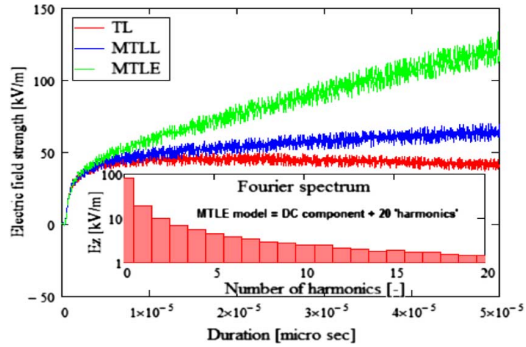

Fig. 2. Vertical electrical-field component sample at 50 m from the strike.

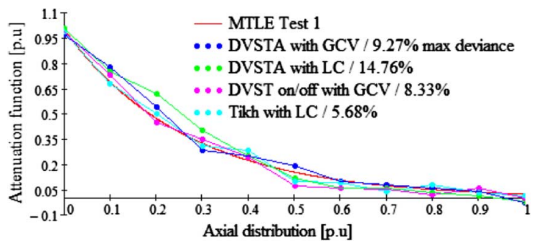

Fig. 3. Inverse reconstruction of the return current spatial distribution with projection and penalty methods.

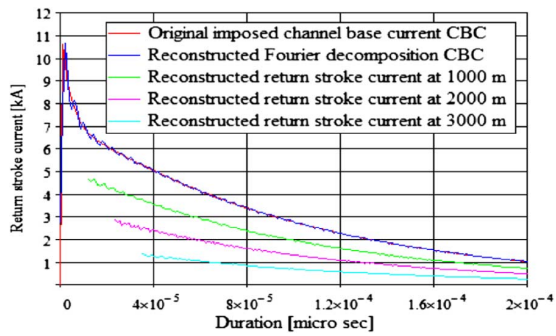

Fig. 4. Return stroke current identification for different attenuation functions.

"harmonics" in not perfectly fitting the CBC (correspondence with the Fourier spectrum of the E_z field), the return stroke current can be evidenced, at different heights, as in Fig. 4. The more "harmonics" that are evaluated, the lower the fluctuation will be in the solution. We assume the model that evidenced discontinuity in the RSC at different heights may be due to dispersion of the current, using the support of [16].

Then, the combination of field equations was then performed, for the scenario with both electric and magnetic measured field components, with only one sensor and applied regularization procedures. A sample of the solution errors yields the optimum approach, for the location of the sensor at 500 m, and MTLE:

In the reconstruction of the MTLL (Test 2) model, we also achieved reasonable performance as related to other reported results [9]–[12]. Regarding the experimental aspects of the present study, it is worth mentioning that we used simulated values as a testing approach. It is our intention to handle also natural or triggered lightning recordings, provided by LINET Germany. More data have to be evaluated in order to adequately validate the models and to improve them in order to reproduce experimental values as closely as possible

We find out that without regularization only for higher frequencies, it is expected to have an improvement in the stability of the solutions, if using single frequency recordings but multiple field sensor locations.

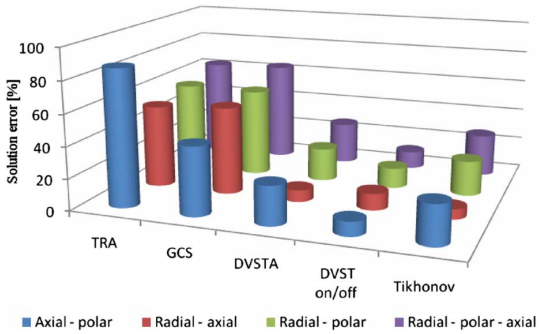

Fig. 5. Sensitive analysis of the regularization applied on the combination of the integral models for a single location electric and magnetic-field sensors.

Using the presented assumptions, we explored the solution behavior for each of the proposed testing conditions. When taking the best frequency spectrum into account, for which to reconstruct the spatial attenuation function, it should be noticed that in the range 1 kHz to 1 MHz (with an additional dc component), the errors reach minimum values.

VI. Concluding Remarks

This paper focuses on the synthesis of lightning return stroke currents, from remotely measured generated fields. After the identification of a mathematical model of the return stroke current, it becomes possible to evaluate the electric- and magnetic-field values in any interest area. Since the problem proves to be severely ill-posed, we proposed a WRA as a group of regularization procedures, all based on the harmonic filtering of the singular vectors.

The effectiveness of the algorithms has been proved especially for ON/OFF DVST and DVSTA; also, for Tikhonov regularization in the combination of two type of field measurements, radial–axial. In order to verify the robustness of the inverse procedure, we added noise to the free term of the system (i.e., to the field measurements).

Although the vertical lightning channel can be acceptable if one does not take into account that real lightning is characterized by tortuosity and branching, one is not able to justify the fine structure of the fields radiated by lightning discharges whose time-domain behavior exhibits a noisy shape with rich spectral [16], [17]. These features, which need further investigations, can be exploited to improve the return stroke current reconstructions.

The author's contribution relates to the introduction and validation of the Fourier frequency decomposition of the field time-domain signals, and numerical regularization in this lightning return stroke current problem reconstruction.

Further activity is in progress on identifying the spatial attenuation and simultaneously finding the time variation and dispersion of the lightning current.

Acknowledgment

This work was supportted in part by the project: "Progress and development through post-doctoral research and innovation in engineering and applied sciences-PRiDE under Contract no. POSDRU/89/1.5/S/57083" under a project co-funded by the European Social Fund through Sectorial Operational Program Human Resources 2007–2013 and in part by the project: "TE 253/2010 Modeling, prediction and design solutions, with maximum effectiveness, for reducing the impact of stray currents on underground metallic gas pipelines." No. 34/2010, under a project funded by the Romanian Ministry of Education.

References

[1] C. Gomes and V. Cooray, "Concepts of lightning return stroke models," *IEEE Trans. Electromagn. Compat.*, vol. 42, no. 1, pp. 82–96, Feb. 2000.

[2] Y. Baba and V. A. Rakov, "Applications of electromagnetic models of the lightning return stroke," *IEEE Trans. Power Del.*, vol. 23, no. 2, pp. 800–811, Apr. 2008.

[3] N. D. Murray, E. P. Krider, and J. C. Willett, "Multiple pulses in the electric field derivative, dE/dt, during the onset of first return strokes in cloud-to-ground lightning," *Atmos. Res.*, vol. 76, pp. 455–458, 2005, Elsevier.

[4] A. Andreotti, U. De Martinis, C. Petrarca, V. A. Rakov, and L. Verolino, "Lightning electromagnetic fields and induced voltages: Influence of channel tortuosity," in *Proc. 30th URSI General Assembly Scientif. Symp.*, Aug. 2011, pp. 1–4.

[5] V. A. Rakov and M. A. Uman, "Review and evaluation of lightning return stroke models including some aspects of their application," *IEEE Trans. Electromagn. Compat.*, vol. 40, no. 4, pt. 2, pp. 403–426, Nov. 1998.

[6] C. A. Nucci, "Lightning-induced voltages on distribution systems: Influence of ground resistivity and system topology," *J. Light. Res.*, vol. 1, pp. 148–157, 2007.

[7] R. Thottappillil, M. A. Uman, and N. Theethayi, "Electric and magnetic fields from a semi-infinite antenna above a conducting plane," *J. Electrostat.*, vol. 61, pp. 209–221, 2004.

[8] V. Cooray and G. Cooray, "The electromagnetic fields of an accelerating charge: Applications in lightning return-stroke models," *IEEE Trans. Electromagn. Compat.*, vol. 52, no. 4, pp. 944–955, Nov. 2010.

[9] A. Andreotti, C. Petrarca, V. A. Rakov, and L. Verolino, "Calculation of voltages induced on overhead conductors by non-vertical lightning channels," *IEEE Trans. Electromagn. Compat.*, vol. 54, no. 4, pp. 860–870, Aug. 2012.

[10] A. Andreotti, D. Asante, S. Falco, and L. Verolino, "An improved procedure for the return stroke current identification," *IEEE Trans. Magn.*, vol. 41, no. 5, pp. 1872–1875, May 2005.

[11] J. C. Willett, D. M. Le Vine, and V. P. Idone, "Lightning return stroke current waveforms aloft from measured field change, current and channel geometry," *J. Geoph. Res.*, vol. 113, pp. 1–45, 2008.

[12] M. Izadi, M. Z. A. Ab Kadir, C. Gomes, and V. Cooray, "Evaluation of lightning return stroke current using measured electromagnetic fields," *Progr. Electromagn. Res.*, vol. 130, pp. 581–600, 2012.

[13] P. C. Hansen, *Discrete Inverse Problems, Insight and Algorithms*. Philadelphia, PA, USA: SIAM, 2010, ch. 2, 5.

[14] O. Chadebec, J.-L. Coulomb, G. Cauffet, and J.-P. Bongiraud, "How to well pose a magnetization identification problem," *IEEE Trans. Magn.*, vol. 39, no. 3, pt. 1, pp. 1634–1637, May 2003.

[15] J. L. Bermudez, F. Rachidi, W. Janischewskyj, V. Shostak, M. Rubinstein, D. Pavanello, A. M. Hussein, J. S. Chang, and M. Paolone, "Determination of lightning currents from far electromagnetic fields: Effect of a strike object," *J. Electrostat.*, no. 65, pp. 289–295, 2007.

[16] Y. Baba and V. A. Rakov, "Electric and magnetic fields predicted by different electromagnetic models of the lightning return stroke versus measured fields," *IEEE Trans. Electromagn. Compat.*, vol. 51, no. 3, pt. 1, pp. 479–487, Aug. 2009.

[17] V. Cooray and V. A. Rakov, "Engineering lightning return stroke models incorporating current reflection from ground and finitely conducting ground effects," *IEEE Trans. Electromagn. Compat.*, vol. 53, no. 3, pp. 773–781, Aug. 2011.

[18] A. Neubauer, "Computation of discontinuous solutions of 2D linear ill-posed integral equations via adaptive grid regularization," *J. Inverse Ill Posed Problems*, vol. 15, no. 1, pp. 99–111, 2007.

[19] U. Tautenhahn, "Regularization of linear ill-posed problems with noisy right hand side and noisy operator," *J. Inverse Ill Posed Problems*, vol. 16, no. 5, pp. 507–524, 2008.

[20] T. Strohmer and R. Vershynin, "A randomized solver for linear systems with exponential convergence," *Proc. RANDOM-APPROX*, vol. 4110, pp. 499–507, 2006.

[21] D. Krawczyk-Stando and M. Rudnicki, "Regularization parameter in discrete ill-posed problems-the use of the U curve," *I.J.A.M. Comput. Sci.*, vol. 17, no. 2, pp. 101–108, 2007.